Journal of Catalysis 270 (2010) 153–162

Contents lists available at ScienceDirect

Journal of Catalysis

journal homepage: www.elsevier.com/locate/jcat

Mechanism of catalytic decomposition of pentachlorophenol by a highly recyclable heterogeneous SiO_2–[Fe-porphyrin] catalyst

Konstantinos C. Christoforidis [a], Maria Louloudi [b], Elena R. Milaeva [c], Yiannis Deligiannakis [a,*]

[a] Laboratory of Physical Chemistry, Department of Environmental and Natural Resources Management, University of Ioannina, Seferi 2, 30100 Agrinio, Greece
[b] Laboratory of Inorganic Chemistry, Department of Chemistry, University of Ioannina, 45100 Ioannina, Greece
[c] Department of Organic Chemistry, Moscow State Lomonosov Univ., Moscow 119992, Russia

ARTICLE INFO

Article history:
Received 24 November 2009
Revised 17 December 2009
Accepted 18 December 2009
Available online 22 January 2010

Keywords:
Heterogeneous catalyst
EPR
DR-UV–Vis
Ferryl
Compound I
High-valent iron
Fe-porphyrin
Immobilized
PCP

ABSTRACT

A novel heterogenized FeR_4P–SiO_2 shows enhanced catalytic efficiency for PCP conversion *vs.* the homogeneous FeR_4P catalyst. The heterogenized FeR_4P–SiO_2 catalyst is highly recyclable in the presence of imidazole in solution. EPR and DR-UV–Vis data provide direct evidence that high-valent iron species $[R_4P^{+\cdot}Fe^{IV}{=}O]$ are formed in the heterogenized FeR_4P–SiO_2 system. The electron spin density of the a_{1u} cation radical ($Por^{+\cdot}$) is mainly localised on the tetrapyrole frame, and this results in the observed weak magnetic coupling between the $S = 1$ oxo-ferryl moiety ($Fe^{IV}{=}O$) and the $S' = 1/2$ porphyrin cation radical ($Por^{+\cdot}$). A catalytic cycle mechanism is suggested. Accordingly, the reduction in $[R_4P^{+\cdot}Fe^{IV}{=}O]$ can proceed *via* a substrate molecule, in a one electron-transfer, thus producing $[R_4PFe^{IV}]$ plus a radical entity derived from the substrate. Then, a second electron-transfer to $[R_4PFe^{IV}]$ leads to the regeneration of the initial R_4PFe^{III} state. This second electron can originate from either a substrate molecule or a radical substrate species.

1. Introduction

Highly chlorinated phenols, such as pentachlorophenol (PCP), have been listed as a priority pollutant by the US Environmental Protection Agency [1] and by European regulatory authorities [2]. Chlorophenols are introduced into the environment as a result of various man-made activities. Because of their broad spectrum of antimicrobial properties, chlorophenols find wide use in pesticides, disinfectants, fungicides, herbicides, insecticides, wood preservatives and many other products. They can are also be present in paper-mill wastes. Although production and use of chlorinated phenols has been banned in several countries [3], chlorophenols – including PCP – are still found in many parts of the world [3,4]. The toxicity and resistance to degradation of chlorophenols increase with the number of halogen substituents [5], a property shared by all chlorinated organic compounds [5]. Thus, due to their resistance to microbial degradation, chlorinated phenols persist for decades in the environment [6]; therefore, efficient catalytic technologies are needed.

Among the competing technologies, oxidative catalysis has been proven very promising. Biological methods suffer from slow rates and limits at high concentrations of pollutants which might become toxic for the biological organisms [7–9]. Advanced oxidation processes such as Fenton and photo-Fenton [2,10–13], photolysis [2,13], ozonation [2,13,14] and photocatalysis [2,15,16] have been widely used for the decomposition of chlorophenols. Non-heme and heme iron enzymes, as well as synthetic iron catalysts are known to oxidise a range of substrates [17–21]. In addition, in the literature of biomimetic degradation of chlorophenols, metaloporphyrin derivative catalysts, mainly Fe-porphyrins [22–24], as well as Mn-porphyrins [25–27] and Co-porphyrins [28] have been used. Fe-porphyrins are far more efficient compared to Mn- and Co-porphyrins [27]. Non-heme iron catalysts were also used, but to a lesser extend [29,30]. Meunier and co-workers used iron tetrasulfophthalocyanine – one of the best water soluble catalysts reported so far – for the catalytic decomposition of TCP and PCP [22]. A highly efficient non-heme iron catalyst for degradation of chlorophenols was reported by Collins and co-workers [30]. Fukushima et al. studied the influence of humic substances on the removal of PCP and the products of the reaction catalyzed by an iron-porphyrin complex [31,32]. In most of these cases, hydrogen peroxide (H_2O_2) or potassium monopersulfate ($KHSO_5$) has been used as primary oxidants. Recently, we have shown that an

* Corresponding author.
E-mail addresses: kchristofo@gmail.com (K.C. Christoforidis), mlouloud@uoi.gr (M. Louloudi), ideligia@cc.uoi.gr (Y. Deligiannakis).

0021-9517/$ - see front matter © 2009 Elsevier Inc. All rights reserved.
doi:10.1016/j.jcat.2009.12.016

iron-porphyrin complex bearing 2,6-di-*tert*-butylphenols at each *meso*-aryl position of the porphyrin ring (herein called FeR_4P, where R = di-Bu^{t}Phen) is very efficient catalyst for PCP degradation in homogeneous phase [33].

An integrated technological design of an efficient catalyst requires among the key-features to be (i) protection against oxidative deactivation due to the rapid self-oxidation [34,35] and (ii) easy recyclability of the catalyst. In heme–iron systems it is generally accepted that increased stability toward oxidative self-destruction, preventing the catalyst deactivation, arises from a combination of electron-withdrawing polar effects in combination with steric hindrance of bulky substituents [36–38]. Thus, the oxidative stability of metallo-tetra-*aryl*-porphyrins benefits by the presence of substituents on the porphyrin ring [39]. For example, the tetrakis(2,6-dichloro- and 2,6-dibromo-phenyl) porphyrins bearing bulky substituents on the *ortho*-positions of the aryl groups [39] have been shown to be effective and robust catalysts [36–38]. Recently, we have shown that FeR_4P – bearing bulky di-*tert*-butylphenols at each *meso*-aryl position – can function catalytically under strong oxidative conditions [33].

Immobilization of the catalyst onto a suitable support has also been suggested to further increase its stability toward the oxidant [40] and to prohibit oxidative degradation by bimolecular interaction [41,42]. Inorganic supports are generally preferred *vs.* organic supports, because they are more robust and more efficient in preventing catalyst deactivation caused by dimerization (e.g. formation of μ-oxo dimmers) [43]. Immobilization is also advantageous in industrial processes, since it facilitates both catalyst separation and recycling and also by diminishing effluent contamination [21]. Immobilization on a suitable support also ensures that only monomeric complexes are responsible for the degradation of the substrate. This can potentially lead to some substrate shape-selectivity, because of specific interactions of the substrates with the inorganic matrix [21]. Thus, immobilization of a Fe-porphyrin catalyst onto a solid inorganic support can provide significant advantages which are in some respects analogous to the influence of the polypeptide chain on hemeproteins [44] e.g. arising from the steric and electronic effects of the support. We, and other research groups, have already made a great deal of efforts on the heterogeneous catalysis, and the results show that they are more efficient than the non-supported catalysts [41,45,46].

In the present work, we present a detailed catalytic and spectroscopic study of a heterogenized catalyst prepared by covalent immobilisation of the iron-porphyrin complex FeR_4P on SiO_2. Our data show that the heterogenized catalyst FeR_4P–SiO_2 is very efficient on the decomposition of PCP. In Fe-porphyrin catalysts, a key reaction-intermediate participating in the catalytic conversion of organic substrates is a high-valent Fe(IV) oxo-porphyrin cation radical complex ([Fe^{IV}=O $Por^{+\cdot}$]) [33,47,48]. However, direct observation of this active specie in heterogenized catalytic systems has not yet been achieved. Herein, we present the first example of a high-valent Fe(IV) oxo-porphyrin cation radical complex ([Fe^{IV}=O $Por^{+\cdot}$]) trapped for the heterogenized FeR_4P–SiO_2 catalyst. This elusive oxidative intermediate specie was studied with UV–Vis and EPR spectroscopy.

In summary, the aims of the present work were (a) to study the catalytic efficiency of the heterogeneous FeR_4P–SiO_2 for decomposition of PCP, (b) to optimise the catalytic conditions for yield and recyclability, (c) to study the catalytic active intermediates of the iron centre.

2. Experimental

All solvents and reagents were of commercial grade unless otherwise stated and were purchased from Merck and Aldrich.

2.1. Metalloporphyrin

The catalyst FeR_4P was synthesized as described previously [49,50] and purified by silica gel column chromatography using $CHCl_3$, 80% $CHCl_3$ and 20% hexane as the eluting solvents [49,50].

2.2. Immobilization

Immobilization of the metalloporphyrin FeR_4P was performed on silica modified by imidazole-3-(glycidyloxypropyl). Detailed description of the procedure used can be found in Refs. [51,52]. In brief: 3-(glycidyloxypropyl)-trimethoxysilane (3 mmol; 0.663 ml) was added to a stirred solution of imidazole (3 mmol; 0.204 g) in 50 ml of toluene. The resulting mixture was heated at 80 °C for 24 h, and after drying, commercial SiO_2 (1.5 g) and EtOH (5 ml) were added. Then, the reaction mixture was stirred at 80 °C for 24 h, producing the modified [imidazole-3-(glycidyloxypropyl)–SiO_2] (herein called IGOPS). The imidazole-functionalized silica (IGOPS) was collected by filtration in vacuum, washed with EtOH and $(CH_3)_2O$ and dried for 12 h. The loading ratio [imidazole-3-(glycidyloxypropyl)]: [IGOPS] achieved was 20% [w:w], determined by thermogravimetric and elemental analysis. The metalloporphyrin (FeR_4P) ligation to IGOPS was achieved by stirring a CH_2Cl_2 solution of a known amount of metalloporphyrin into a suspension of IGOPS for 24 h. The powder supported catalyst (FeR_4P–SiO_2) was washed with CH_2Cl_2 – to remove unbound and weakly bound porphyrin – and dried for 3 h at 60 °C. The loadings were quantified by measuring (UV–Vis) the amount of unloaded metalloporphyrin or by measuring the iron by Atomic Absorption Spectrometry in a Perkin–Elmer A700 GFAAS.

2.3. UV–Vis spectroscopy

Light absorbance spectra in the ultraviolet–visible region (190–900 nm) were recorded by using a double-beam Perkin–Elmer Lambda-35 UV–Vis spectrophotometer using 10-mm quartz cells. Diffuse-Reflectance (DR) UV–Vis spectra were recorded using a Perkin–Elmer Micro-DRS system. The system provides excellent S/N for sample quantities 5–10 mg.

2.4. EPR spectroscopy

Electron Paramagnetic Resonance (EPR) spectra were recorded using a Brucker ER200D spectrometer at liquid N_2 temperatures, equipped with an Agilent 5310A frequency counter. The spectrometer was running under a home-made software based on LabView [33].

2.5. HPLC analysis

Quantitative HPLC determinations for PCP were performed using a Dionex P680 HPLC chromatograph equipped with a Dionex 1024 Diode Array Detector. The column used was Acclaim C18 5 μM, 120 Å, 4.6 × 250 mm and was thermostated at 23 °C. The HPLC mobile phase was a mixture of an aqueous (Milli-Q) solution of 0.8% H_3PO_4 and acetonitrile (15/85 v/v) with a flow rate of 1 ml/min. Under this experimental setup, PCP was measured at 7.5 min retention time and at 210 nm.

2.6. Samples for studies of reaction intermediates: UV–Vis sample preparation

The liquid samples were prepared in 10-mm quartz cells. A typical reaction mixture contained 2.965 ml of acetonitrile (CH_3CN), 5 μl of 6 mM FeR_4P stock solution in CH_2Cl_2 (i.e. 10 μM), 15 μl of 20 mM imidazole i.e. [Cat:Imid] = 1/10 and 10 μM of $NaIO_4$ (i.e.

1 equiv. of $NaIO_4$ with respect to the FeR_4P complex). In all samples, appropriate volumes of Milli-Q water were added to a final ratio [CH_3CN:H_2O] of [100:1]. The oxidation of the solid samples was performed by the addition of small amount (i.e. 5 μl) of 10 μM $NaIO_4$ aqueous CH_3CN (1:1 v/v) stock solution to the surface of the powder sample. This method applied for the oxidation of the solid catalyst can not be used for quantitative analysis; however, it allows the observation of active intermediates as it will be shown in Section 3.4.1.

2.7. EPR sample preparation

All EPR samples were prepared in quartz tubes of 5-mm internal diameter. Appropriate volumes of 60 mM imidazole aqueous stock solution were added (a) in 90 μl of 6 mM homogeneous FeR_4P solution in CH_2Cl_2 and (b) in 54 μl of CH_2Cl_2 containing 5 mg of the heterogenized FeR_4P–SiO_2 complex (i.e. the corresponding concentration of was FeR_4P 1 mM) – so that the final ratio [catalyst:imidazole] was [1:10] – followed by incubation for 30 min. For the oxidation of the samples, $NaIO_4$ was used as oxidant. The two samples (homogeneous FeR_4P and heterogenized FeR_4P–SiO_2) were oxidised by the addition of appropriate volumes of 280 mM $NaIO_4$ aqueous stock solution, so that the final [$NaIO_4$] was 28 mM, followed by incubation for 30 min. The solution potential measured at the beginning of the reaction was 250–270 mV. In the present work, all measurements were taken using the following conditions unless otherwise mentioned: liquid nitrogen (77 K) or helium (4.2 K) temperature, 100 kHz modulation frequency, 10 G modulation amplitude and 10 dB microwave power.

2.8. Catalytic procedures

All reactions were performed in test tubes of 4 ml equipped with a magnetic stirrer at room temperature. A typical reaction mixture contained 187.5 μM PCP (100 μl of a 3.75 mM acetonitrile stock solution), 18.7 μM of the catalyst (0.0032 g of the immobilized or 970 μl of a 38.5 μM acetonitrile stock solution of the homogeneous catalyst i.e. catalyst: substrate ratio = 10%), 2.34 mM of the oxidant (23.4 μl of a 200 mM $NaIO_4$ aqueous stock solution i.e. 12.5 equiv. of oxidant with respect to the substrate), 187 μM or 37.5 μM μl of imidazole as co-catalyst (37.4 μl and 7.5 μl, respectively, of 10 mM aqueous stock solution i.e. 10 or 2 equiv., respectively, of imidazole with respect to the catalyst). For all reactions tested, the appropriate volumes of acetonitrile and Milli-Q water were added, so that the final volume of the reaction was 2 ml, and the ratio acetonitrile:H_2O equals to 3:1, v:v, unless otherwise mentioned. We selected this solvent mixture (acetonitrile:H_2O 3:1), because FeR_4P is only soluble in non-polar solvents. Acetonitrile was also used as co-solvent to solubilize the hydrophobic PCP. In all cases, the oxidant was the last reagent added. The quantification of PCP by HPLC was based on comparison with standards.

2.9. Recycling of the catalyst

After the first use of the catalyst, the solid phase catalyst was separated by centrifugation; then, the catalyst was washed extensively using acetonitrile according to the following procedure: 3 ml of acetonitrile was added to the catalyst and was magnetically stirred for 10 min. The mixture was centrifuged, and the solvent was removed. This procedure was repeated three times. Finally, the remained solvent was evaporated, and the dried powder was collected. No mechanical treatment was used to dry the powder catalyst. EPR spectra were collected after the procedure described above to quantify the presence of the Fe-centres on the recycled catalyst.

3. Results and discussion

3.1. Catalytic decomposition of PCP

Catalytic PCP conversion data by the heterogenized SiO_2–FeR_4P/$NaIO_4$ system studied in a mixture of CH_3CN:H_2O (3:1 v/v) are shown in Table 1.

According to Table 1, for [catalyst:PCP:$NaIO_4$] = [1:10:125] within 2.5 h at room temperature, PCP was 100% converted by the heterogeneous system (run **1**). For comparison, within 2.5 h at room temperature, the homogeneous FeR_4P catalyst was able to convert only a 7% of PCP (Table 1, run **5**). Increase in the [catalyst:PCP] ratio to [1:100] resulted to a 50% and 100% decomposition of the substrate within 2.5 and 24 h, respectively, by the heterogenized catalyst (Table 1, run **4**).

Control experiments were run as follows: a control reaction using SiO_2–IGOPS e.g. with no FeR_4P porphyrin, resulted in zero PCP conversion (data not shown). In both heterogeneous and homogeneous FeR_4P catalytic systems, no conversion of PCP was

Table 1
Oxidation of PCP by $NaIO_4$ catalyzed by homogeneous FeR_4P and heterogenized FeR_4P–SiO_2.

Run	% PCP/oxidant*	% Cat/PCP	% Cat/Imid**	% PCP Conversion		
				20 min	2.5 h	24 h
Heterogeneous FeR_4P–SiO_2 system						
1	12.5	10	–	20	100	–
2	12.5	10	50	24	100	–
3	12.5	10	10	26	100	–
4	12.5	1	50	7	50	100
Homogeneous FeR_4P system						
5	12.5	10	–	1.5	7	26
6	12.5	10	10	3.5	10	30

*Oxidant = $NaIO_4$, **Imid = imidazole.

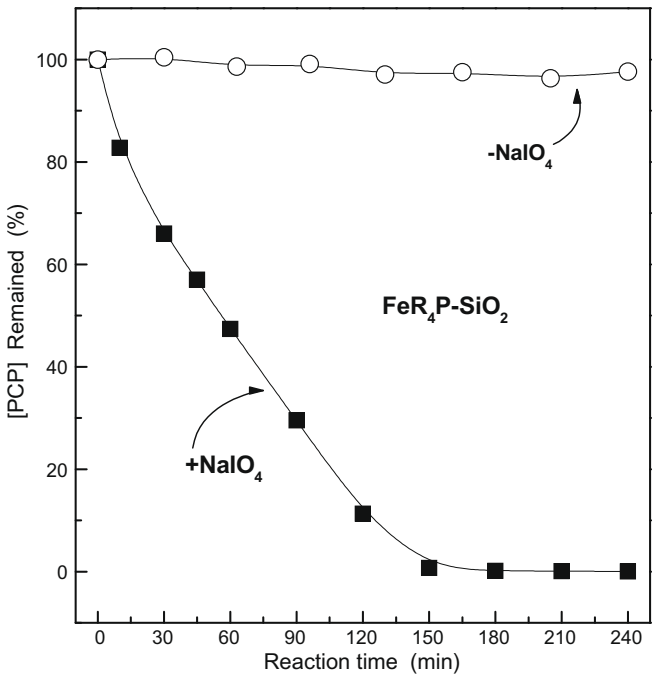

Fig. 1. Catalytic decomposition of PCP by the FeR_4P–SiO_2/$NaIO_4$ system. The reactions were performed in a 3:1 mixture of CH_3CN:H_2O. Conditions: [Cat:PCP:oxidant] = [1:10:125]. (■) run **1** (see Table 1) with $NaIO_4$, (○) as in run **1** without oxidant (reference reaction).

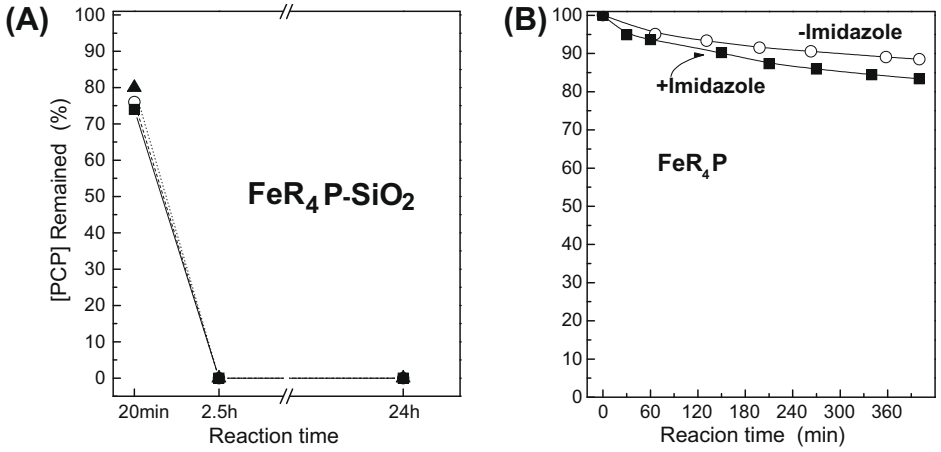

Fig. 2. Effect of imidazole addition on the decomposition of PCP: (A) by the *heterogeneous FeR$_4$P–SiO$_2$/NaIO$_4$ system*. Run **1** [Cat:Imid:PCP:NaIO$_4$] = [1:0:10:125] (doted line, ▲), run **2** [Cat:Imid:PCP:NaIO$_4$] = [1:2:10:125] (dashed line, ○) and Run **3** [Cat:Imid:PCP:NaIO$_4$] = [1:10:10:125] (solid line, ■). (B) By the *homogeneous FeR$_4$P/NaIO$_4$ system*: run **5** [Cat:Imid:PCP:NaIO$_4$] = [1:0:10:125] (○), run **6** [1:10:10:125] (■).

observed within 24 h, when no chemical oxidant was added to the reaction mixture (Fig. 1). The kinetics of the catalytic reaction in Fig. 1 shows a complex pattern, which cannot fit by a single kinetic term. EPR spectroscopy provides evidence for some degree of catalyst degradation *via* the formation of the "free" Fe^{III} signal at $g = 4.3$ [33]. Using this information, under the conditions of Fig. 1, ~5% of the catalyst was degraded.

3.1.1. Effect of imidazole on PCP conversion

When imidazole was used at a ratio of 10:1 with respect to the homogeneous catalyst, [Imid:FeR$_4$P] = [10:1], the catalytic decomposition of PCP was increased by 14% within a period of 24 h, see Fig. 2B. In striking contrast, imidazole had a much smaller effect on the decomposition of PCP by the heterogenized FeR$_4$P–SiO$_2$ catalyst, Fig. 2A. More particularly, as shown in Fig. 2A, imidazole enhanced slightly the rate PCP of decomposition only at the beginning of the reaction, i.e. at 20 min. However, imidazole had no effect at longer reactions times, i.e. 2.5 h. The data in Fig. 2A and B reveal that imidazole in solution is enhancing the catalytic activity of FeR$_4$P only in the homogeneous phase [33]. The heterogenized FeR$_4$P–SiO$_2$ has a high efficiency which is only marginally benefited by dissolved imidazole.

As we show in the following (Section 3.3.1), in the heterogenized system, an imidazole is coordinating the Fe-centre i.e. *via* the imidazole-functionalized silica (IGOPS) moiety, therefore boosting the catalytic efficiency of the FeR$_4$P–SiO$_2$ with no need for added imidazole in solution.

In addition, it is possible that surface-bound imidazoles, not coordinated by FeR$_4$P centres, might influence the catalytic activity of the heterogenized catalyst. Our data show that 2.9 mmoles of unbound imidazole exists per gram of FeR$_4$P–SiO$_2$ material. According to the data for the homogeneous FeR$_4$P [see also [33]], imidazoles in solution – not coordinated to the FeR$_4$P – play a cocatalytic role in the catalysis of PCP. In this context, it might be considered that surface-bound imidazoles in the near vicinity of surface FeR$_4$P centres might play a "cocatalytic" role in the catalytic activity of the heterogenized catalyst. This issue is further analysed in Section 3.2.1 in the discussion of recyclability experiments discussed in the following.

3.2. Recycling of the FeR$_4$P–SiO$_2$ catalyst

To evaluate the stability of the catalyst, recycling experiments were carried out, and the results are summarised in Table 2. For each new cycle, the catalyst was separated from the reaction mixture, washed extensively, dried and re-used under the same experimental conditions. Fig. 3 shows 3D plots of the effect of [catalyst:imidazole] ratio (*X*-axes) and the catalyst re-uses (*Y*-axes) on the conversion of PCP (*Z*-axes).

Table 2
Oxidation of PCP by NaIO$_4$ catalyzed by the heterogenized iron(III) porphyrin (FeR$_4$P–SiO$_2$). Initial concentrations: [FeR$_4$P] = 18.7 μM, [PCP] = 187.5 μM, [NaIO$_4$] = 2.34 mM.

Run		[Imid] (μM)	PCP conversion (%)		
			20 min	2.5 h	24 h
1	*1st use*	–	*20*	*100*	*100*
	2nd use	–	*7*	*55*	*88*
	3rd use	–	*4*	*18*	*69*
	Total PCP converted		***31***	***173***	***257***
2	*1st use*	*37.5*	*24*	*100*	*100*
	2nd use	*37.5*	*11*	*100*	*100*
	3rd use	*37.5*	*5*	*22*	*86*
	Total PCP converted		***40***	***222***	***286***
3	*1st use*	*187*	*26*	*100*	*100*
	2nd use	*187*	*18*	*100*	*100*
	3rd use	*187*	*7*	*27*	*98*
	Total PCP converted		***51***	***227***	***298***
Reference reactions					
No catalyst		*187*	–	–	–
No oxidant		*187*	–	–	–

According to Table 2 and Fig. 3, when no imidazole was used, a gradual decrease in the catalytic activity was observed upon recycling the catalyst. For example, at reaction time 2.5 h, the conversion of PCP achieved was 100%, 55% and 18%, respectively, for the 1st, 2nd and 3rd use of the catalyst under the conditions of run **1** (Fig. 3B, Table 2). However, when imidazole was used as co-catalyst, PCP conversion remained high, see Fig. 3 and Table 2.

More particularly, after 2.5 h, the FeR$_4$P–SiO$_2$ catalyst retained high (100%) catalytic activity on the 1st and 2nd usage when imidazole was used as co-catalyst, (Fig. 3B, runs **2** and **3**). On its 3rd usage within 2.5 h, the efficiency of the catalyst showed some decrease; however, the catalytic efficiency was fully retained after 24 h. More specifically, within 2.5 h (24 h) 22 (86)% and 27 (98)% of PCP was decomposed in the 3rd re-use, runs **2** and **3**, respectively (compare Fig. 3B and C).

The loss of the catalyst material due to separation and cleaning process was carefully estimated to be less than 6.2% after the 3rd use relative to the initial material, based on the weight of the catalyst. Therefore, the loss of the catalyst-mass after every use is

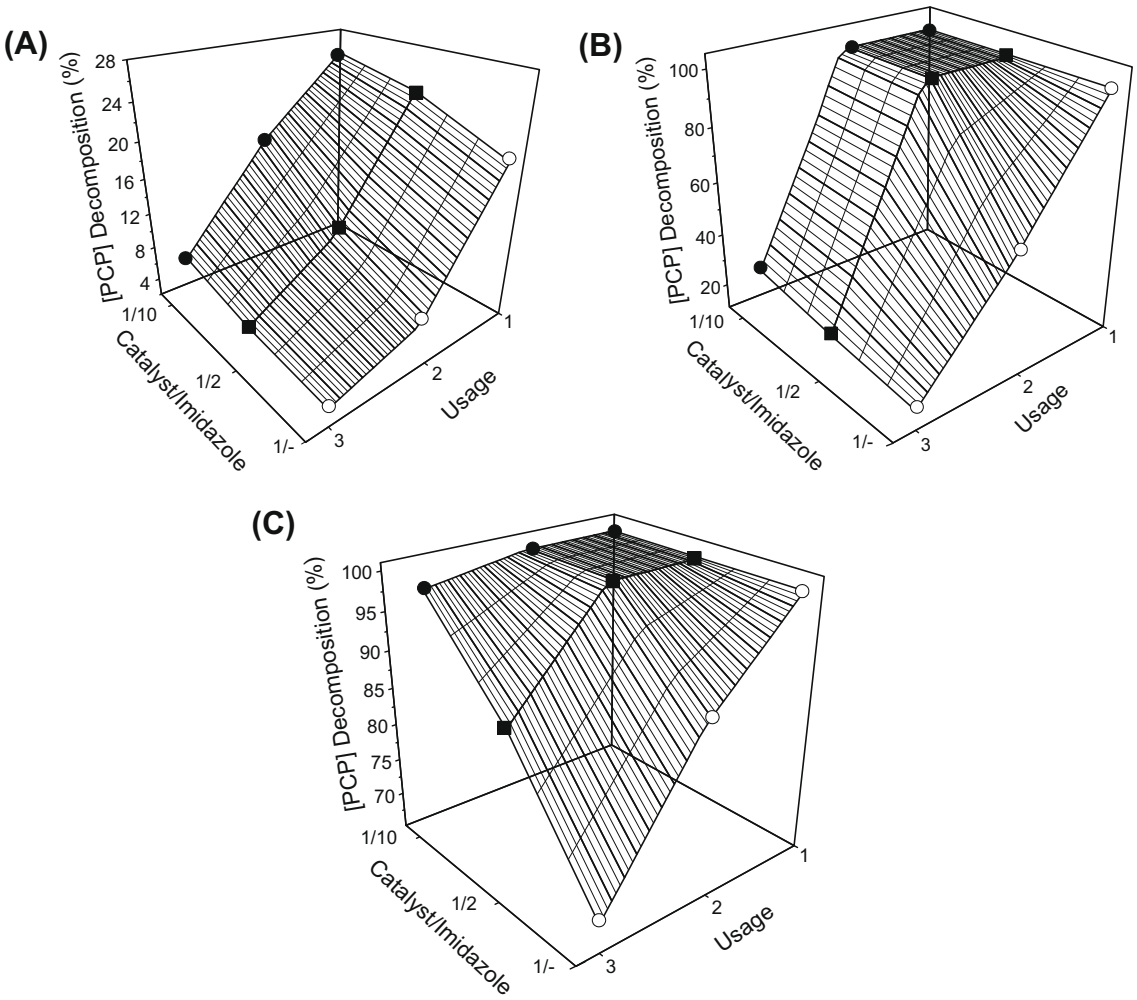

Fig. 3. Effect of the [catalyst:imidazole] ratio and catalyst re-uses on the conversion of PCP at (A) 20 min, (B) 2.5 h, and (C) 24 h. *Catalytic conditions*: [Cat:Imid} = [1/–] (○ – run **1**), [1:2] (■ – run **2**) and [1:10] (● – run **3**). In all experiments, [Cat:PCP:$NaIO_4$] = [1:10:125].

estimated to be on average ~3%. Hence, mass-loss would explain only a small decrease in the catalytic activity after each usage. This shows that the relatively high decrease in catalytic activity upon re-use of the catalyst, observed when no imidazole was added (Fig. 3, run **1**), is not due to mass-loss. Instead, deactivation of the FeR_4P–SiO_2 catalyst may occur in the absence of added imidazole in solution.

EPR spectra, collected after each use of the catalyst, revealed that after the 3rd use of the catalyst with no imidazole present, increased amounts of non-specific high-spin Fe^{III} signal at g 4.3 were developed (data not shown). The g 4.3 signal indicates that the iron was detached from the R_4 porphyrin frame. Thus, after the repetitive use of catalysts, described in Fig. 3, the kinetics gets more complex involving the intermediate steps as well as catalyst degradation to an increasing degree.

Overall, the present EPR and catalytic data demonstrate that in the absence of added imidazole, deactivation of the recycled FeR_4P–SiO_2 catalyst may occur under the catalytic conditions tested herein *via* reactions which destroy the active FeR_4P complex releasing Fe^{III} ions.

3.2.1. Effect of imidazole on the recyclability of FeR_4P–SiO_2

According to Table 2 and Fig. 3, imidazole has a remarkable beneficial effect on the stability, as well as on the efficiency of the FeR_4P–SiO_2/$NaIO_4$ system for PCP decomposition. This can be easily observed at the third usage of the catalyst at *t* 24 h (Fig. 3C), where a progressive increase in the catalytic activity is observed with increasing imidazole concentration.

Overall, the present data reveal an intriguing phenomenon: although imidazole does not improve the catalytic performance at the first usage of the catalyst, the presence of imidazole is obligatory for further re-use of the catalyst in order to achieve complete decomposition of PCP (Fig. 3C). In the presence of imidazole, remarkable reusability and efficiency are achieved for the FeR_4P–SiO_2 catalyst.

It is possible that surface-bound imidazoles, not bound by FeR_4P centres, might play some cocatalytic role in the catalytic activity of the heterogenized catalyst. In this respect, progressive loss of these surface-bound imidazoles – during the repetitive catalytic cycles – might be related to the observed loss of catalytic activity of the re-used FeR_4P–SiO_2 catalyst. This bears pertinence to the observation that imidazole added in the catalytic solution can act as a co-catalyst e.g. counter-balancing the role of lost surface-bound imidazoles. This mechanism also explains the observation that added imidazole in solution is required only after the repetitive uses of the FeR_4P–SiO_2 catalyst.

3.3. Catalytic active intermediates: EPR study of the high-spin Fe^{III} ($S = 5/2$) to low-spin Fe^{III} ($S = 1/2$) conversion

Fig. 4 shows low-temperature (77 K) EPR spectra of the homogeneous (spectra (a) and (e)), the heterogeneous (spectrum (d))

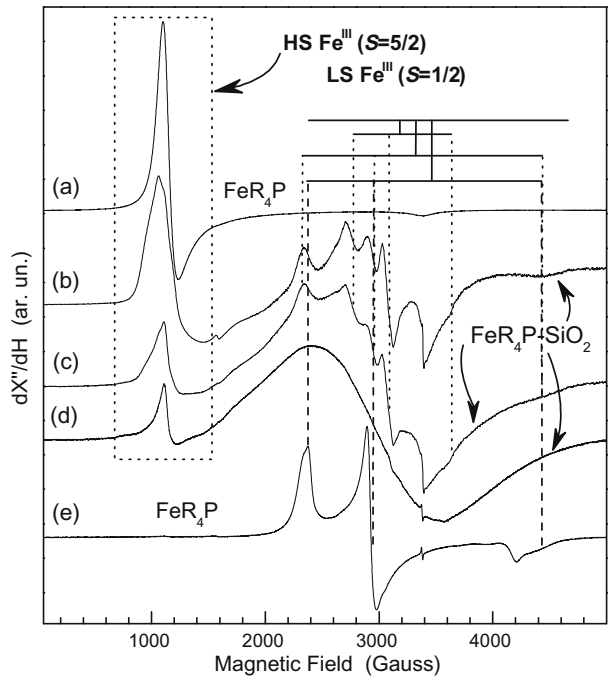

Fig. 4. Low-temperature EPR spectra (a) for the homogeneous FeR_4P catalyst in CH_2Cl_2, (b) for FeR_4P incubated with IGOPS in CH_2Cl_2 for $t = 3$ h, and (c) for FeR_4P incubated with IGOPS in CH_2Cl_2 $t = 24$ h. Spectrum (d) corresponds to heterogeneous FeR_4P–SiO_2 catalyst powder obtained after drying. Spectrum (e) corresponds to the homogeneous SiO_2–FeR_4P incubated in CH_2Cl_2 for 30 min in the presence of 10 equiv. of imidazole *vs.* FeR_4P.

and the homogeneous adsorbed on IGOPS–SiO_2 (spectra (b) and (c)). Spectrum (a) corresponds to the homogeneous (FeR_4P) catalyst in CH_2Cl_2. The EPR spectrum is characterized by an axial EPR signal with g-values $g_x = 6.13$, $g_y = 5.77$, $g_z = 1.99$ [33], typical for high-spin (HS) Fe^{III}-porphyrin complexes ($S = 5/2$) [33]. Spectrum (e) corresponds to the homogeneous FeR_4P catalyst incubated for 30 min with 10 equiv. of imidazole with respect to the iron-porphyrin complex.

The three-line pattern in spectrum (e) is characteristic of rhombically distorted Fe^{III} at the low-spin (LS) state ($S = 1/2$). As shown recently [33], the rhombic g-values ($g_x = 2.86$, $g_y = 2.3$, $g_z = 1.56$) are typical for two axially coordinated imidazoles. This EPR signal is demonstrating that in the homogeneous FeR_4P complex, the presence of 10 equiv. of imidazole (*vs.* FeR_4P) converts all the Fe-centres from the high-spin ($S = 5/2$) to the low-spin Fe^{III} ($S = 1/2$) state [33].

On going to the heterogenized SiO_2–FeR_4P powder, spectrum (d) in Fig. 4, we observe that the EPR spectrum is characterized by a small HS Fe^{III} fraction ($S = 5/2$) and a broad derivative signal centered at 3000 G with a line-width of 1000 G. In order to understand the nature of this broad signal, the interaction of homogeneous FeR_4P complex with imidazole-functionalized silica (IGOPS) was studied in detail by monitoring the time evolution of the EPR signals, during the preparation of the heterogeneous catalyst (FeR_4P–SiO_2) in CH_2Cl_2.

3.3.1. Formation of the FeR_4P–SiO_2 complex in CH_2Cl_2

The EPR spectra (b) and (c) in Fig. 4 show the interaction of FeR_4P with IGOPS in CH_2Cl_2 after 3 h (b) and 24 h (c). At short reaction times $t < 10$ min, the EPR spectrum is identical to spectrum (a) in Fig. 4 (data not shown). This is the EPR spectrum of FeR_4P in solution before to get attached on the IGOPS. After 3 h, the interaction of FeR_4P with IGOPS in CH_2Cl_2 results in formation of LS Fe^{III} ($S = 1/2$) signals at the expense of the HS signals, see spectrum (b). After 24 h, only 20% of the FeR_4P centres were remaining in the high-spin Fe^{III} state i.e. see spectrum (c). We have carefully verified that simple adsorption of FeR_4P on SiO_2 does not affect the HS signals, and no low-spin EPR signals were generated (data not shown). This demonstrates that IGOPS is responsible for the conversion of the iron to the LS state, observed in spectra (b) and (c). Analysis of the EPR spectra in Figs. 4 reveals that at least three different LS Fe^{III} species (herein called LS^a, LS^b, LS^c) can be resolved in the EPR spectra (b) and (c) for FeR_4P plus IGOPS. The g-values as well as the rhombicity (V/Δ) and tetragonality (Δ/λ) parameters [33,53] of the observed LS Fe^{III} species are listed in Table 3. This shows that coordination of the iron by the imidazole ring of IGOPS can adopt more than one conformation relative to the porphyrin ring [53]. Prolonged incubation of the FeR_4P plus IGOPS sample (i.e. 24 h) leads to a broader EPR spectrum (spectrum (c)). The g-value distribution results in progressively broader EPR signals for the low-spin iron centres. Taking all these observations together, we consider that the broad derivative EPR signal of the heterogeneous FeR_4P–SiO_4 in the powder sample, spectrum (d), reflects a distribution of LS Fe^{III} ($S = 1/2$) EPR signals. The data show that (i) g-value heterogeneity e.g. due to different orientation of the FeR_4P complex with respect to the plane of the axial coordinated imidazole molecule [53] and (ii) line broadening from magnetic interactions between nearby paramagnetic centres is responsible for the severe line broadening of the low-spin Fe^{III} EPR signals in the FeR_4P–SiO_4 powder.

Importantly, the data in Fig. 4 show that in the FeR_4P–SiO_4 powder, the iron centres have been converted to the low-spin state with *no* need for additional imidazole. Using the EPR spectra (a) and (e), we estimate that for the heterogeneous FeR_4P–SiO_2 sample, spectrum (d) corresponds to a HS/LS ratio of 20% and 80%, respectively. As a control, incubation of the heterogeneous FeR_4P–SiO_2 powder with 10 equiv. of imidazole in CH_2Cl_2 did not cause any changes on the features of the EPR spectrum (data no shown).

3.4. Catalytic active intermediates: formation of the [Fe^{IV}=O $Por^{+\cdot}$] state for the heterogeneous SiO_2–FeR_4P catalyst

The formation of high oxidation states of the Fe-centres was monitored by EPR and UV–Vis spectroscopy.

3.4.1. UV–Vis spectroscopy

Fig. 5A presents Diffuse-Reflectance UV–Vis spectra for powder heterogenized FeR_4P–SiO_2 catalyst. The band at 424 nm corresponds to the Soret band of the iron-porphyrin complex immobilized on silica [54] (Fig. 5A solid line). Upon the addition of 5 μl of 10 μM $NaIO_4$ aqueous solution, the Soret band began to decrease, and a new well-defined peak at the visible area was generated at 665 nm (Fig. 5A dashed line).

For comparison, the solid line in Fig. 5B shows the absorption spectrum of the homogeneous complex FeR_4P incubated with 10 equiv. of imidazole for 10 min (solid line). Upon oxidation with 1 equiv. of $NaIO_4$, the color of the solution turned to green, the Soret band decreased, and a peak at 665 nm appeared (Fig. 5B dashed line). All these changes in the visible spectra of both samples are

Table 3
EPR spectral parameters of the low-spin species in FeR_4P–SiO_4.

Specie	g_x	g_y	g_z	Δ/λ	V/Δ
LS^a	2.89	2.29	1.55	3.20	0.63
LS^b	2.71	2.21	1.52	3.15	0.68
LS^c	2.58	2.0	1.82	5.50	0.59
$FeR_4P[Imid]_2$	2.86	2.0	1.56	3.01	0.67

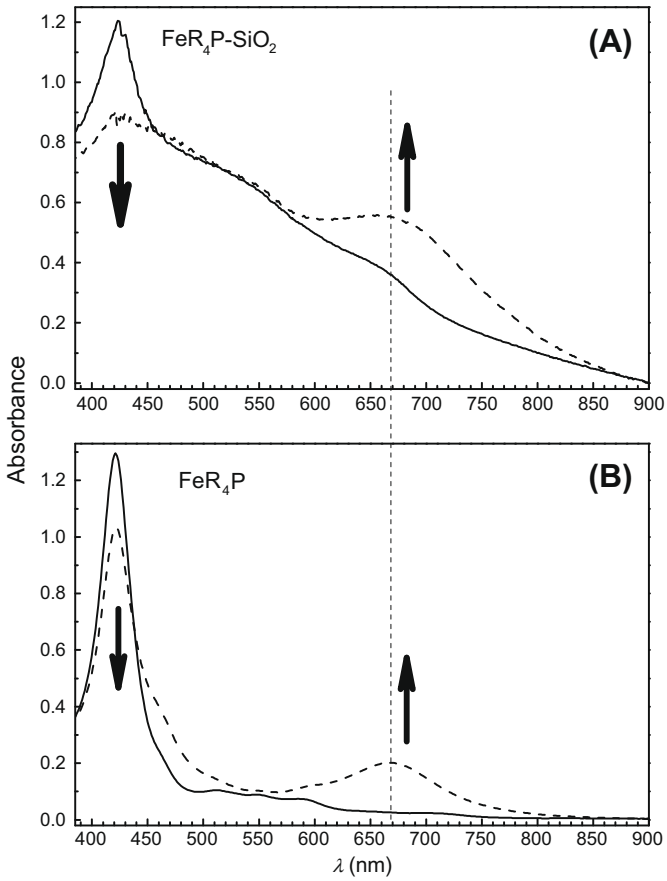

Fig. 5. (A) DR-UV–Vis spectra for the heterogenized catalyst (FeR_4P–SiO_2) without $NaIO_4$ (solid line) and upon oxidation with $NaIO_4$ (dashed line). (B) UV–Vis spectra for homogeneous catalyst (FeR_4P) with 10 equiv. of imidazole in CH_3CN (solid line) and upon oxidation with 1 equiv. on $NaIO_4$ (dashed line).

characteristic for the formation of an oxo-Fe^{IV} porphyrin π-cation radical specie (ferryl porphyrin π-cation radical, (Fe^{IV}=O $Por^{+\cdot}$) [54–57]. The green color is characteristic of the Fe^{IV}=O $Por^{+\cdot}$ specie [33,58–60]. Accordingly, in the oxidised heterogeneous FeR_4P–SiO_2 catalyst, the transient signal at 665 nm is assigned to the Fe^{IV}=O $Por^{+\cdot}$ specie.

In both heterogeneous and homogeneous samples, the transient band at 665 nm decreased gradually, the rate of decrease being faster for increased concentrations of $NaIO_4$ (data not shown). To the best of our knowledge, this is the first experimental observation of the Fe^{IV}=O $Por^{+\cdot}$ specie in heterogenized Fe-catalyst with UV–Vis spectroscopy.

Fujii and co-workers [57] showed, that among other factors, the axial ligand influences the electronic properties to Fe-porphyrins which resemble Compound I of peroxidases and catalases [57]. In [57], it was shown that the band at around 650 nm may be a good comparative marker of the electron donor ability of the axial ligand. In this context, imidazole was found to be among the most drastic electron donor ligands [57] in model Fe-porphyrin complexes. The data in Fig. 5 show that for both the homogeneous FeR_4P and the heterogeneous FeR_4P–SiO_2 catalyst, the band at 665 nm is developed by the formation of Fe^{IV}=O $Por^{+\cdot}$ state. Accordingly, the UV–Vis data show that in both systems, the electron donor ability of the axial imidazoles should be comparable. Otherwise stated, the electron donor ability of the imidazole of the IGOPS in the FeR_4P–SiO_2 catalyst is comparable to the electron donor ability of the axial imidazole in the FeR_4P in solution. As suggested in [57,61], the effect of the axial ligand is correlated with the electronic state (a_{1u} or a_{2u}) of the porphyrin π-cation radical in the Fe^{IV}=O $Por^{+\cdot}$ state. In porphyrins forming an a_{1u} state i.e. like FeR_4P [33], axial imidazole accelerates the formation of Fe^{IV}=O $Por^{+\cdot}$ state as well as oxo-transfer to the substrate during the catalytic cycle [57,62]. This issue was further clarified herein by using EPR spectroscopy.

3.4.2. EPR spectroscopy

As described in Section 3.3.1, the EPR spectra of the heterogenized catalyst contained mainly low-spin Fe^{III}. Oxidation of the FeR_4P–SiO_2 sample with 28 mM $NaIO_4$ resulted in a gradual decrease in the Fe^{III} signals. After incubation for 15 min with $NaIO_4$, they became undetectable. Importantly, after 25 min, a new EPR signal developed consisted by a broad signal at $g \sim 3.68$ and a sharp feature near g 2, see Fig. 6 spectrum (b). In a similar way, in the homogeneous FeR_4P complex, within 15 min after the addition of oxidant (28 mM $NaIO_4$), the low-spin EPR signal was zeroed, with a concomitant development of a broad signal at $g \sim 3.41$ and a sharp feature at g 2, see Fig. 6 spectrum (d). All these changes in the EPR spectra of both samples bear relevance to previously reported EPR spectra of heme enzymes [63–67] or model Fe-porphyrin systems [68,69] under comparable conditions and are characteristic for the formation of a ferryl porphyrin π-cation radical specie (Fe^{IV}=O $Por^{+\cdot}$).

The data in Fig. 6b show the first example of a [$R_4P^{+\cdot}Fe^{IV}$=O] oxidation state observed for a heterogenized iron-porphyrin system. The EPR spectral characteristics of the [$R_4P^{+\cdot}Fe^{IV}$=O] in both the homogeneous and the heterogeneous catalysts can be attributed to a system of two weakly coupled electron spins. The interaction of the two electron spins is derived from a $S = 1$ oxo-ferryl moiety (Fe^{IV}=O) magnetically coupled with a $S' = 1/2$ porphyrin cation radical ($Por^{+\cdot}$) [63–71]. This interaction corresponds to porphyrins forming an a_{1u} state [57]. In the a_{1u} state, the electron spin density of the cation radical ($Por^{+\cdot}$) is mainly localised on the tetrapyrole frame, and this results in the observed weak magnetic coupling between the $S = 1$ oxo-ferryl moiety (Fe^{IV}=O) and the $S' = 1/2$ porphyrin cation radical ($Por^{+\cdot}$).

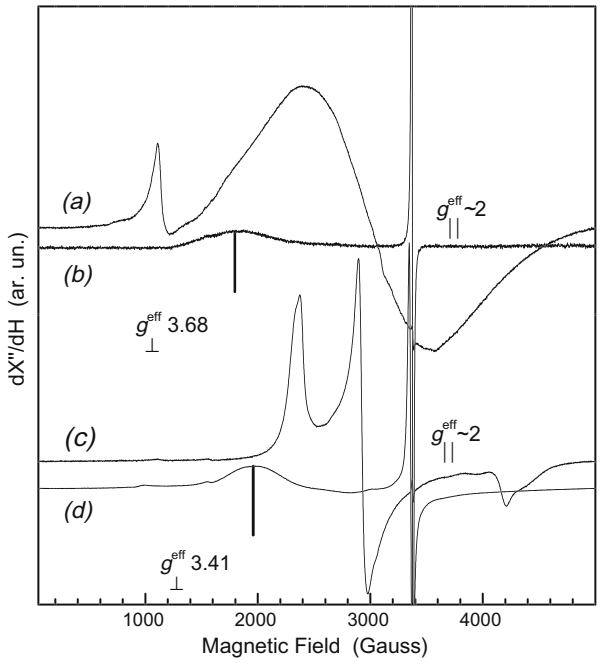

Fig. 6. EPR spectra of (a) the heterogenized catalyst (FeR_4P–SiO_2) in CH_2Cl_2 and (b) incubated for 30 min with 28 mM $NaIO_4$. (c) 6 mM of the homogeneous catalyst (FeR_4P) in CH_2Cl_2 incubated for 30 min with 10 equiv. of imidazole and (d) incubated for 30 min with 28 mM $NaIO_4$.

As analysed previously [57,72], for oxoiron (IV) porphyrin complexes, two unpaired electrons in the d_π orbitals of ferryl (Fe^{IV}=O) iron i.e. the d_{xz} and d_{yz} delocalise into the imidazole π-orbital e.g. the highest occupied π-orbital of the imidazole [57,72]. On the other hand, the spin of the π-orbital of the porphyrin cation radical ($Por^{+\cdot}$), for symmetry reasons, could be transferred to the sigma (σ) orbital of the axial imidazole *via* the unoccupied d_z^2 orbital of the ferryl (Fe^{IV}=O) iron. In a_{1u} radical complexes, like the [$R_4P^{+\cdot}Fe^{IV}$=O] in Fig. 6, weak coupling between the spins of porphyrin cation radical ($Por^{+\cdot}$) and the ferryl (Fe^{IV}=O) iron results in small spin-transfer to the axial imidazole.

The coupling between the spins of porphyrin cation radical ($Por^{+\cdot}$) and the ferryl (Fe^{IV}=O) iron can be quantified from the EPR signals as follows: the magnetic coupling is determined by both exchange and dipolar terms [64,67]. This coupling scheme was first proposed to explain the EPR signal centered at $g \sim 2$ for Horseradish Peroxidase Compound I [64]. Since then, analogous EPR spectra were discovered and interpreted analogously in Lignin Peroxidase [63] and Chloroperoxidase [66] as well as in synthetic systems [57,68,69] and recently for the homogeneous [$R_4P^{+\cdot}Fe^{IV}$=O] oxidation state [33].

The EPR signals can be interpreted by assuming a weakly coupled pair of spin s Fe^{IV}=O ($S = 1$) and $Por^{+\cdot}$ ($S' = 1/2$). The coupling is assumed to be a weak exchange interaction J [64,67,71]. Within the formalism of the weakly coupled ($S = 1$ and $S' = 1/2$) system, the [Fe^{IV}=O $Por^{+\cdot}$] is characterized by three Kramer's doublets separated by energy gaps which are mainly determined by the value of D, that is the zero-field splitting of the $S = 1$ state of Fe^{IV}=O [56,64,67]. Since for the ferryl porphyrin centre, D is expected to be greater than zero [56,64,67,71], a value for $g_\perp$ that is greater than $g_{||}$ results from ferromagnetic coupling [67,71].

$$g_\perp > g_{||} \quad J > 0 \text{ (ferromagnetic coupling)}$$

The value of $g_\perp^{eff}$ is determined by the exchange interaction with the ferryl moiety ($S = 1$). To a first approximation [67,71]

$$\begin{aligned} g_{||}^{eff} &\sim g_e \\ g_\perp^{eff} &\sim g_e + 2g_\perp^{Fe}(J/D) \end{aligned} \quad (1)$$

where $g_\perp^{Fe}$ is associated with the isolated [Fe^{IV}=O]^{II} moiety and can be taken equal to 2.25 [73], and J/D is the ratio of exchange coupling to the zero-field splitting parameter of [Fe^{IV}=O]^{II}. Using Eq. (1) and the g-values of the heterogeneous and homogeneous sample from the EPR spectra (b) and (d) in Fig. 6, respectively, it follows

$$\frac{|J|}{D} = 0.37 \quad (2)$$

for the heterogeneous catalyst (FeR_4P–SiO_2) and

$$\frac{|J|}{D} = 0.31 \quad (3)$$

for the homogeneous catalyst (FeR_4P) with $J > 0$, i.e. ferromagnetic coupling.

For both samples, the observed $|J|/D$ values are similar to those reported by Fujii et al. for their a_{1u} radical state of TMTMP–iron-porphyrin complexes with axial imidazole [57,71]. A detailed analysis of the spin Hamiltonian parameters based on for the temperature dependence of the EPR signals e.g. as described in [33] gives J = +5.2 K and D = 16.7 K for the homogeneous catalyst. In the heterogeneous catalyst, D = 16.7 K, J = +6.2 K. In general, both the ratio J/D as well as the J values show little change between the homogeneous [$R_4P^{+\cdot}Fe^{IV}$=O] and the heterogeneous SiO_2–[$R_4P^{+\cdot}Fe^{IV}$=O] state.

If we take into account that the small changes can be accounted for by differences in IGOPS (in the heterogenized catalyst) *vs.* imidazole (in the homogeneous) coordination, as shown in Section 3.3.1., this leads to the important conclusion that the SiO_2 matrix does not perturb the [$R_4P^{+\cdot}Fe^{IV}$=O] state. Overall, the detailed comparison of the EPR data for the homogeneous *vs.* the heterogeneous catalyst shows that the SiO_2 matrix does not perturb the [$Fe^{III}R_4P$] or the [$R_4P^{+\cdot}Fe^{IV}$=O] state. Structurally, this can be attributed to the long chain of the IGOPS which holds the immobilized FeR_4P molecules remotely from the SiO_2 surface. This important conclusion shows that the improved catalytic performance in not due to changes induced by the SiO_2 matrix.

3.5. Catalytic-mechanistic considerations

The oxidation of $Fe^{III}R_4P$ by $NaIO_4$, which is an efficient oxygen atom donor, generates the active oxidant for PCP degradation. Based on our spectroscopic data, in both systems (homogeneous and heterogeneous), this active intermediate was identified as an oxo-Fe^{IV} porphyrin π-cation radical [$R_4P^{+\cdot}Fe^{IV}$=O] [33], similar to Compound I of heme enzymes.

Fig. 7 shows possible pathways for the reduction in the high-valent specie formed, together with the corresponding EPR spectrum for each step observed during the catalytic cycle of the catalyst. At the beginning of the suggested mechanism, PCP molecules are considered to be in their protonated PCP—OH form. During the catalytic cycle, see steps B and C in Fig. 7, PCP is deprotonated by the active [Fe^{IV}=O $Por^{+\cdot}$] or [Fe^{IV}=O Por] intermediates i.e. generating a transient PCP radical. According to our data, two alternative paths may be suggested for the reduction in this high-valent specie, see Fig. 7:

(i) As described by step B in Fig. 7, the reduction in [$R_4P^{+\cdot}Fe^{IV}$=O] can proceed *via* a substrate molecule, in a one electron-transfer, thus producing [R_4PFe^{IV}] (Compound II) plus a radical entity derived from the substrate. Then, a second electron-transfer to [R_4PFe^{IV}] leads to the regeneration of the initial R_4PFe^{III} state. This second electron can originate from either a substrate molecule (step C) or a radical substrate species (step D). In Fig. 7, the suggested catalytic cycle A–B–C for our system bears strong relevance to the catalytic cycle suggested by Fukushima et al. [32]. However, in the present work, the active intermediate specie of the catalyst responsible for the catalytic PCP oxidation was observed and identified experimentally, while no direct evidence was provided for the catalytic [Fe(III)-porphyrin/$KHSO_5$] system used for the oxidation of PCP in Ref. [32].

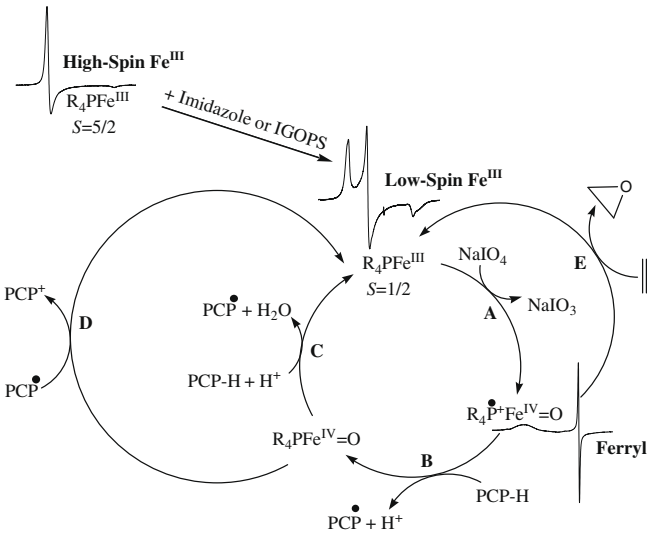

Fig. 7. Possible reaction mechanisms involved in the $Fe^{III}R_4P/NaIO_4$/PCP system.

(ii) Alternatively, the oxo-Fe^{IV} porphyrin cation radical specie $[R_4P^{+\cdot}Fe^{IV}=O]$ is able to transfer the oxygen atom on a suitable substrate molecule i.e., an olefinic double bond, by a two electron-transfer step, see step E in Fig. 7. This would regenerate the initial R_4PFe^{III} state *via* step E [52]. However, recently, it has been shown that the oxidative transformation of chlorinated phenols by chloroperoxidase involves two consecutive one-electron steps from the two forms $[Fe^{IV}=O\ Por^{+\cdot}]$ (Compound I) and $[Fe^{IV}=O\ Por]$ (Compound II) rather than a single two-electron oxidation [74]. Based on the structural relationship between our system and the one in Ref. [74] as well as their application on the same substrate, it may be suggested that the first path (i) is more likely to take place in the present study.

3.6. Structure–catalytic function relationship

Our catalytic experiments have shown that the catalytic activity of the homogeneous catalyst for the decomposition of PCP is enhanced in the presence of imidazole as additive. The increase in the catalytic performance of the homogeneous system in the presence of imidazole can be attributed to the axial ligation of imidazole playing the role of the proximal His residue in enzymes. In contrary, the heterogenized $FeR_4P–SiO_4$ catalyst has been shown to be independent of imidazole as an additive in solution. This is because (a) the attachment of $Fe^{III}R_4P$ on silica e.g. IGOPS was performed with an imidazole spacer through the formation of a $Fe–N_{imidazole}$ coordination bond (b) surface-bound imidazoles, not coordinated by FeR_4P centres, might play a cocatalytic role. This treatment benefits the obtained heterogeneous $Fe^{III}R_4P–SiO_2/NaIO_4$ system with the advantage of the axial imidazole ligation producing a heterogeneous system independent on the external imidazole addition. Moreover, the SiO_2 matrix does not perturb the $[Fe^{III}R_4P]$ or the $[R_4P^{+\cdot}Fe^{IV}=O]$ state, which can be attributed to the long chain of the IGOPS. By comparing the two systems, it can be seen that the heterogenized catalyst is more efficient and rapid on the catalytic decomposition of PCP. Furthermore, it is highly reusable. This can be attributed to the resistance against the oxidative destruction due to the inorganic support. The immobilization of the FeR_4P catalyst through the axial ligation of an imidazole molecule and the enhanced resistance against oxidative destruction result in the rapid and complete conversion of PCP by the heterogeneous $Fe^{III}R_4P/NaIO_4$ system.

4. Conclusions

The heterogenized $FeR_4P–SiO_2$ shows enhanced catalytic efficiency for PCP conversion *vs.* the homogeneous Fe R_4P catalyst. The heterogenized $FeR_4P–SiO_2$ catalyst is highly recyclable in the presence of imidazole in solution.

In both the homogeneous and the heterogeneous FeR_4P catalysts, our EPR and DR-UV–Vis data provide direct evidence that high-valent iron species $[R_4P^{+\cdot}Fe^{IV}=O]$ are formed. This is the first literature report the detection of high-valent iron species in heterogenized iron-porphyrin catalyst. In the active state a_{1u} state of the $Por^{+\cdot}$ the electron spin density of the cation radical ($Por^{+\cdot}$) is mainly localised on the tetrapyrole frame, and this results in the observed weak magnetic coupling between the $S = 1$ oxo-ferryl moiety ($Fe^{IV}=O$) and the $S' = 1/2$ porphyrin cation radical ($Por^{+\cdot}$).

EPR data for the homogeneous *vs.* the heterogeneous catalyst show that the SiO_2 matrix does not perturb the $[Fe^{III}R_4P]$ or the $[R_4P^{+\cdot}Fe^{IV}=O]$ state. Structurally, this can be attributed to the long chain of the IGOPS which holds the immobilized FeR_4P molecules remotely from the SiO_2 surface.

A catalytic cycle mechanism is suggested. Accordingly, the reduction in $[R_4P^{+\cdot}Fe^{IV}=O]$ can proceed *via* a substrate molecule, in a one electron-transfer, thus producing $[R_4PFe^{IV}]$ plus a radical entity derived from the substrate. Then, a second electron-transfer to $[R_4PFe^{IV}]$ leads to the regeneration of the initial R_4PFe^{III} state. This second electron can originate from either a substrate molecule or a radical substrate species.

Acknowledgment

This work has been supported by a NATO Grant GBP.EAP.CLG983239.

References

[1] L.H. Keith, W.A. Telliard, Environ. Sci. Technol. 13 (1979) 416.
[2] M. Pera-Titus, V. Garcia-Molina, M.A. Banos, J. Gimenez, S. Esplugas, App. Catal. B 47 (2004) 219.
[3] S.R. Wild, S.J. Harrad, K.C. Jones, Chemosphere 24 (1992) 833.
[4] J. Muir, G. Eduljee, Sci. Total Environ. 236 (1999) 41.
[5] M. Alexander, Science 211 (1981) 132.
[6] B. Meunier, A. Sorokin, Acc. Chem. Res. 30 (1997) 470.
[7] T. Hatta, O. Nakano, N. Imai, N. Takizawa, H. Kiyohara, J. Biosci. Bioeng. 87 (1999) 267.
[8] N. Pal, G. Lewandowski, P.M. Armenante, Biotechnol. Bioeng. 46 (1995) 599.
[9] K.A. McAllister, H. Lee, J.T. Trevors, Biodegradation 7 (1996) 1.
[10] M. Fukushima, K. Tatsumi, Environ. Sci. Technol. 35 (2001) 1771.
[11] W.Z. Tang, C.P. Huang, Chemosphere 33 (1996) 1621.
[12] R. Oliveira, M.F. Almeida, L. Santos, L.M. Madeira, Ind. Eng. Chem. Res. 45 (2006) 1266.
[13] F.J. Benitez, J. Beltran-Hereida, J.L. Acero, F.J. Rubio, Chemosphere 41 (2000) 1271.
[14] F.J. Benitez, J. Beltran-Hereida, J.L. Acero, F.J. Rubio, Ind. Eng. Chem. Res. 38 (1999) 1341.
[15] G. Mills, M.R. Hoffmann, Environ. Sci. Technol. 27 (1993) 1681.
[16] J.P. Wilcoxon, J. Phys. Chem. B 104 (2000) 7334.
[17] E. Nordlander, A.M. Whalen, F. Prestopino, Coord. Chem. Rev. 146 (1995) 225.
[18] E.I. Solomon, T.C. Brunold, M.I. Davis, J.N. Kemslay, S.K. Lee, N. Lehnert, F. Neese, A.J. Skulan, Y.S. Yang, J. Zhou, Chem. Rev. 100 (2000) 235.
[19] M. Costas, M.P. Mehn, M.P. Jensen, L. Que, Chem. Rev. 104 (2004) 939.
[20] X. Shan, L. Que, J. Inorg. Biochem. 100 (2006) 421.
[21] D. Mansuy, Coord. Chem. Rev. 125 (1993) 129.
[22] A. Sorokin, J.L. Seris, B. Meunier, Science 268 (1995) 1163.
[23] A. Sorokin, S. Suzzoni-Dezard, D. Poullain, J.-P. Noel, B. Meunier, J. Am. Chem. Soc. 118 (1996) 7410.
[24] G. Lente, J.H. Espenson, New J. Chem. 28 (2004) 847.
[25] Q. Labat, J.-L. Seris, B. Meunier, Angew. Chem. Int. Ed. Engl. 29 (1990) 1471.
[26] S. Rismayani, M. Fukushima, A. Sawada, H. Ichikawa, K. Tatsumi, J. Mol. Catal. A 217 (2004) 13.
[27] A. Sorokin, B. Meunier, Chem. Eur. J. 2 (1996) 1308.
[28] B. Agboola, K.I. Ozoemena, T. Nyokong, J. Mol. Catal. A: Chem. 227 (2005) 209.
[29] C. Hemmert, M. Renz, B. Meunier, J. Mol. Catal. A 137 (1999) 205.
[30] S.S. Gupta, M. Stadler, C.A. Noser, A. Ghosh, B. Steinhoff, D. Lenoir, C.P. Horwitz, K.-W. Schramm, T.J. Collins, Science 296 (2002) 326.
[31] M. Fukushima, H. Ichikawa, M. Kawasaki, A. Sawada, K. Morimoto, K. Tatsumi, Environ. Sci. Technol. 37 (2003) 386.
[32] M. Fukushima, A. Sawada, M. Kawasaki, H. Ichikawa, K. Morimoto, K. Tatsumi, Environ. Sci. Technol. 37 (2003) 1031.
[33] K.C. Christoforidis, M. Louloudi, E.R. Milaeva, Y. Sanakis, Y. Deligiannakis, Mol. Phys. 105 (2007) 2185.
[34] R.A. Sheldon (Ed.), Metalloporphyrins in Catalytic Oxidations, Marcel Dekker, New York, 1994.
[35] M.J. Nappa, C.A. Tolman, Inorg. Chem. 24 (1985) 4711.
[36] P.S. Traylor, D. Dolphin, T.G. Traylor, J. Chem. Soc., Chem. Commun. 5 (1984) 279.
[37] D. Ostovic, T.C. Bruice, J. Am. Chem. Soc. 111 (1989) 6511.
[38] M.D. Assis, J.R.L. Smith, J. Chem. Soc., Perkin Trans. II 10 (1998) 2221.
[39] B. Meunier, Chem. Rev. 92 (1992) 1411.
[40] C. Crestini, A. Pastorini, P. Tagliatesta, J. Mol. Catal. A: Chem. 208 (2004) 195.
[41] M.S.M. Moreira, P.R. Martins, R.B. Curi, O.R. Nascimento, Y. Iamamoto, J. Mol. Catal. A: Chem. 233 (2005) 73.
[42] P.R. Cooke, J.R. Lindsay-Smith, Tetrahedron Lett. 33 (1992) 2737.
[43] T. Tatsumi, M. Nakamura, H. Tominaga, Catal. Today 6 (1989) 163.
[44] A.W. Van, J.W.H. der Made, R.J.M. Smeets, W. Nolte, W. Drenth, J. Chem. Soc., Chem. Commun. 21 (1983) 1204.
[45] B. Fu, P. Zhao, H.C. Yu, J.W. Huang, J. Liu, L.N. Ji, Catal. Lett. 127 (2009) 411.
[46] Y. Iamamoto, Y.M. Idemori, S. Nakagaki, J. Mol. Catal. A: Chem. 99 (1995) 187.
[47] S.J. Yang, W. Nam, Inorg. Chem. 37 (1998) 606.
[48] K.A. Lee, W. Nam, J. Am. Chem. Soc. 119 (1997) 1916.
[49] L.R. Milgrom, C.C. Jones, A. Harriman, J. Chem. Soc., Perkin Trans II 1 (1988) 71.

[50] T.G. Traylor, K.B. Nolan, R. Hildreth, J. Am. Chem. Soc. 105 (1983) 6149.
[51] M. Louloudi, K. Mitopoulou, E. Evaggelou, Y. Deligiannakis, N. Hadjiliadis, J. Mol. Catal. A: Chem. 198 (2003) 231.
[52] E.R. Milaeva, O.A. Gerasimova, A.L. Maximov, E.A. Ivanova, E.A. Karachanov, N. Hadjiliadis, M. Louloudi, Catal. Commun. 8 (2007) 2069.
[53] F.A. Walker, B.H. Huynh, W.R. Scheidt, S.R. Osvath, J. Am. Chem. Soc. 108 (1986) 5288.
[54] J.T. Groves, R.C. Haushalter, M. Nakamura, T.E. Nemo, B.J. Evans, J. Am. Chem. Soc. 103 (1981) 2884.
[55] M.D. Assis, O.A. Serra, Y. Iamamoto, O.R. Nascimento, Inorg. Chim. Acta 187 (1991) 107.
[56] H. Fujii, T. Yoshimura, H. Kamada, Inorg. Chem. 36 (1997) 6142.
[57] A. Takahashi, T. Kurahashi, H. Fujii, Inorg. Chem. 48 (2009) 2614.
[58] M. Sono, J.H. Dawson, J. Biol. Chem. 257 (1982) 5496.
[59] R.H. Felton, G.S. Owen, D. Dolphin, J.J. Fajer, J. Am. Chem. Soc. 93 (1971) 6332.
[60] R.H. Felton, G.S. Owen, D. Dolphin, A. Forman, D.C. Borg, J. Fajer, Ann. N.Y. Acad. Sci. 206 (1973) 504.
[61] H. Fujii, J. Am. Chem. Soc. 115 (1993) 4641.
[62] K. Yamaguchi, Y. Watanabe, I. Morishima, J. Am. Chem. Soc. 115 (1993) 4058.
[63] A. Khindaria, A.D. Aust, Biochemistry 35 (1996) 13107.
[64] C.E. Schulz, P.W. Devaney, H. Winkler, P.G. Debrunner, N. Doan, R. Chiang, R. Rutter, L.P. Hager, FEBS Lett. 103 (1979) 102.
[65] C.E. Schulz, R. Rutter, J.T. Sage, P.G. Debrunner, L.P. Hager, Biochemistry 23 (1984) 4743.
[66] R. Rutter, L.P. Hager, H. Dhonau, M. Hendrich, M. Valentine, P. Debrunner, Biochemistry 23 (1984) 6809.
[67] J.E. Roberts, B.M. Hoffman, R. Rutter, L.P. Hager, J. Am. Chem. Soc. 103 (1981) 7654.
[68] S. Nagakaki, Y. Iamamoto, O. Baffa, O.R. Nascimento, Inorg. Chim. Acta 186 (1991) 39.
[69] Y. Iamamoto, M. das D. Assis, O. Baffa, S. Nakagaki, O.R. Nascimento, J. Inorg. Biochem. 52 (1993) 191.
[70] J.T. Groves, R. Quinn, T.J. McMurray, M. Nakamura, G. Lang, B. Bose, J. Am. Chem. Soc. 107 (1985) 354.
[71] H. Fujii, T. Yoshimura, H. Kamada, Inorg. Chem. 35 (1996) 2373.
[72] A.L. Balch, G.N. La Mar, L. Latos-Grazynski, M.W. Renner, V. Thanabal, J. Am. Chem. Soc. 107 (1985) 3003.
[73] B.M. Hoffman, J.E. Roberts, C.H. Kang, E. Margoliash, J. Biol. Chem. 256 (1981) 6556.
[74] R.L. Osborne, M.K. Coggins, J. Terner, J.H. Dawson, J. Am. Chem. Soc. 129 (2007) 14838.